Contribution from the Department of Chemistry,
The University of Western Ontario, London, Ontario, Canada N6A 5B7

π-Cation-Radical Formation following Visible Light Photolysis of Porphyrins in Frozen Solution Using Alkyl Chlorides or Quinones as Electron Acceptors

ZBIGNIEW GASYNA, WILLIAM R. BROWETT, and MARTIN J. STILLMAN*

Received July 24, 1984

The photochemical oxidation of tetratolylporphine, H_2TPP, tetraphenylporphine, H_2TPP, and ZnTPP and MgTPP metalloporphyrins has been investigated at low temperature in frozen solutions by using alkyl chlorides as "irreversible" or quinones as "reversible" electron acceptors. The oxidized products of the photolysis have been characterized by optical absorption and EPR spectroscopies as porphyrin π cation radicals. The differences in the $ZnTPP^{+\cdot}$ absorption spectra, especially in the 650-nm region, suggest a spectral dependence on the type of acceptor used. Quenching of the porphyrin luminescence has been found to occur in rigid frozen solutions containing either alkyl chloride or quinone acceptors. Both the accumulation of the porphyrin π-cation-radical species and the quenching of the porphyrin luminescence are due to a one-electron photooxidation reaction that is interpreted in terms of a long-range electron-transfer mechanism. An excellent correlation was obtained between $\ln (I/I_0)$ for emission intensity and the concentration of the acceptor, which clearly indicates that the quenching efficiency relates to the efficiency of electron transfer; the efficiency can also be estimated by consideration of the energetics for the reaction. The decay curves of the porphyrin fluorescence were found to deviate significantly from a single exponential decay, when the porphyrin was in the presence of the acceptor. A generalized nonexponential decay function is proposed for the analysis of the decay curves to account for a competitive quenching of the porphyrin fluorescence by the electron-transfer reaction.

Introduction

It is well-known that low-energy excited states of porphyrins can be involved in electron-transfer reactions from the porphyrin to an acceptor molecule, yielding the charge-separated products. In two previous papers[1,2] we reported that photoinduced, one-electron oxidation of porphyrins takes place readily for several different porphyrins in alkyl chloride solvents both at room temperature[1] and in low-temperature glasses.[2] The photolysis of the porphyrins at low temperature in glassy solutions results in the charge-separated reaction species that are trapped in the rigid glass and are stable for several hours. Although the photochemical oxidation of porphyrins to the cation-radical product has been previously reported for samples as frozen solutions by either UV irradiation or photooxidation of charge-transfer complexes,[3-5] none of these methods have been found to be appropriate as a synthetic route to the formation of a single species at high yield, which is a necessary precondition for a detailed photophysical characterization of the reaction products.

Many different types of porphyrin–quinone (the so called PQ) molecules, where the porphyrin and quinone are held in more or less rigid orientations at various center-to-center distances, have been synthesized in order to study the effects of distance and orientation on the electron-transfer reaction between the excited porphyrin donor and the quinone acceptor, e.g. $P^*\cdot\cdot Q \rightarrow P^{+\cdot}\cdot\cdot Q^{-\cdot}$.[6-13] Although attempts have been made to stabilize the radical of both the metal-free and metallated porphyrins in these linked porphyrin–quinone systems,[11,12] less than 5% of the linked porphyrin could be converted to the oxidized porphyrin π-cation-radical species. The high rate of the back-electron-transfer reaction for the linked PQ molecule apparently prevents a steady-state charge separation from being maintained, although in the studies of a flexibly linked PQ molecule[11,12] a longer-lived, charged-separated species is formed than would be predicted from energetic arguments alone. The efficiency of the charge separation should depend on the thermodynamic conditions for both the forward electron-transfer reaction, which involves the excited states of the porphyrin, and the back-electron-transfer reaction between the ground-state radical ions, as well as on a spatial orientation effect that will control overlap of the two sets of molecular orbitals.

While optical and magnetic circular dichroism (MCD) spectra clearly indicate that systematic changes take place in the porphyrin π-electron system following one-electron π-ring oxidation of metalloporphyrins,[1,14] the optical changes observed with the oxidation of the metal-free porphyrin compounds are not well-known. In particular, optical absorption spectra for the very unstable (in room-temperature solutions) cation-radical species obtained from the D_{2h}, metal-free tetratolyl- or tetraphenylporphyrins have not been determined, yet these species are central to the chemistry of the PQ species currently being examined.

In this paper, we describe the characterization of the photooxidation products of metal-free tetratolyl- and tetraphenylporphyrins and the zinc and magnesium metalated complexes of tetraphenylporphyrin obtained in frozen solutions containing alkyl chloride electron acceptors. In addition, we have investigated the photoinduced reactions of a system that models the PQ type of molecules by using a mixture of nonlinked ZnTPP with a variety of quinone molecules embedded in a rigid matrix. For this system we are able to show clearly that accumulation of the ZnTPP π-cation-radical species follows photolysis and that the yield depends on the type of quinone used. The quenching of the steady-state fluorescence and phosphorescence of ZnTPP in this system, as well as the change of the fluorescence decay kinetics in the presence of the quinone, is interpreted as being due to the quenching of the excited ZnTPP states by a competitive electron-transfer reaction.

Experimental Section

H_2TTP, H_2TPP, ZnTPP, and MgTPP were synthesized according to published procedures.[15] Reagent grade 1,1,2,2-tetrachloroethane, TCE (Fisher), was purified by treatment with several changes of concentrated sulfuric acid, washed with sodium hydroxide and water, and finally distilled under nitrogen. Tetramethylsilane, Me_4Si (MSD Isotopes),

(1) Gasyna, Z.; Browett, W. R.; Stillman, M. J. *Inorg. Chem.* **1984**, *23*, 382.
(2) Gasyna, Z.; Browett, W. R.; Stillman, M. J. *Inorg. Chim. Acta* **1984**, *92*, 37.
(3) Bobrovskii, A. P.; Kholmogorov, V. E. *Opt. Spectrosc. (Engl. Transl.)* **1971**, *30*, 17.
(4) Sidorov, A. N. *Biophysics (Engl. Transl.)* **1974**, *19*, 44.
(5) Umrikhin, V. A.; Gribova, Z. P. *Biophysics (Engl. Transl.)* **1974**, *19*, 651.
(6) Loach, P. A.; Runquist, J. A.; Kong, J. L. Y.; Dannhauser, T. J.; Spears, K. G. In "Electrochemical and Spectrochemical Studies of Biological Redox Components"; Kadish, K. M., Ed.; American Chemical Society: Washington, DC, 1982; ACS Symp. Ser. No. 201, pp 515–561.
(7) Migita, M.; Okada, T.; Mataga, N.; Nishitani, S.; Kurata, N.; Sakata, Y.; Misumi, S. *Chem. Phys. Lett.* **1981**, *84*, 263.
(8) Netzel, T. L.; Bergkamp, M. A.; Chang, C.-K.; Dalton, J. *J. Photochem.* **1981**, *17*, 451.
(9) Harriman, A.; Hosie, R. J. *J. Photochem.* **1981**, *15*, 163.
(10) Connolly, J. S. In "Photochemical Conversion and Storage of Solar Energy"; Rabani, J., Ed.; The Weizman Science Press of Israel: Jerusalem, 1982; Part A, pp 175–204.
(11) McIntosh, A. R.; Siemiarczuk, A.; Bolton, J. R.; Stillman, M. J.; Ho, T.-F.; Weedon, A. C *J. Am. Chem. Soc.* **1983**, *105*, 7215.
(12) Siemiarczuk, A.; McIntosh, A. R.; Ho, T.-F.; Stillman, M. J.; Roach, K. J.; Weedon, A. C.; Bolton, J. R.; Connolly, J. S. *J. Am. Chem. Soc.* **1983**, *105*, 7224.
(13) Lindsey, J. S.; Mauzerall, D. C.; Linschitz, H. *J. Am. Chem. Soc.* **1983**, *105*, 6528.
(14) Browett, W. R.; Stillman, M. J. *Inorg. Chim. Acta* **1981**, *49*, 69.
(15) Fuhrhop, J. H. In "Porphyrins and Metalloporphyrins"; Smith, K. M., Ed.; Elsevier: Amsterdam, 1975; pp 757–869.

0020-1669/85/1324-2440$01.50/0

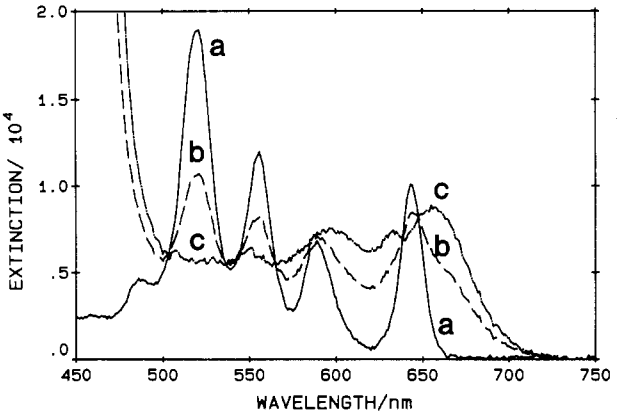

Figure 1. Optical absorption spectra of (a) H_2TPP, (b) photolysed H_2TPP, and (c) $H_2TPP^{+\cdot}$ (calculated) in BuCl–TCE (1:1 v/v) at 79 K. The spectrum of the radical was calculated from the spectra of the irradiated and nonirradiated porphyrin solutions on the basis of an estimated 62% photolytic conversion.

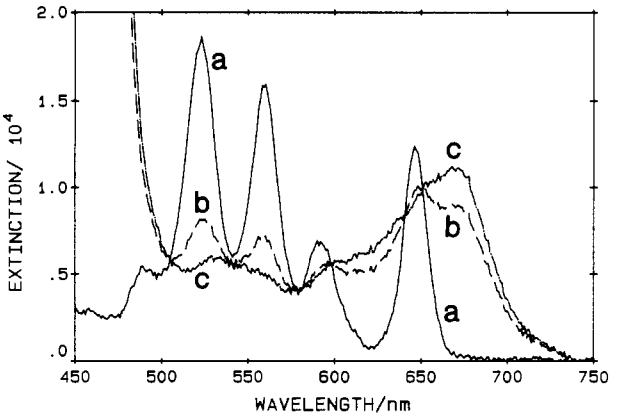

Figure 2. Optical absorption spectra of (a) H_2TPP, (b) photolysed H_2TPP, and (c) $H_2TTP^{+\cdot}$ (calculated) in BuCl–TCE (1:1 v/v) at 79 K. The spectrum of the radical was calculated from spectra of the irradiated and nonirradiated porphyrin solutions on the basis of an estimated 70% photolytic conversion.

reagent grade 2-chlorobutane, BuCl (BDH), and spectranalyzed CCl_4 (Fisher) were used without further purification. Reagent grade *p*-benzoquinone, BQ (Fisher), tetrachloro-*p*-benzoquinone, *p*-Cl_4Q (Baker), tetrachloro-*o*-benzoquinone, *o*-Cl_4Q (Aldrich), and 2,3-dichloro-5,6-dicyanobenzoquinone, DDQ (Kodak) were purified by either recrystallization or sublimation. 2-Methyltetrahydrofuran, MTHF (Aldrich), was freshly distilled to remove the BHT inhibitor.

The porphyrins were dissolved in an appropriate solvent to which the acceptor was added; the solution was placed in an optical cell, which was then plunged into liquid nitrogen in order to prepare the glass. The cell was quickly transferred into an Oxford Instruments CF204 cryostat, and the optical absorption spectra were recorded on a Cary 219 spectrophotometer. The temperature, which was controlled by means of an Oxford Instruments CLTS probe mounted on the cryostat connected to an Oxford Instruments Model DTC2 temperature controller, was maintained within +0.1 K during the measurements. The absorption spectra were automatically digitized, the base lines, which were recorded for solvents in the absence of the porphyrin, were subtracted from the spectra of the samples, and the resulting spectra were replotted using a computer. A 300-W tungsten–halogen Kodak projector lamp, controlled by a variable transformer, was used for the photolysis of the samples. The light was filtered through appropriate Corning filters. Only light with wavelength >400 nm was used.

The EPR spectra were recorded on a Varian E-12 EPR spectrometer equipped with a Varian E-257 temperature controller and interfaced to a Nicolet 1180 computer through a Nicolet Explorer III digital oscilloscope. For EPR measurements, porphyrin solutions were transferred to 4-mm o.d. tubes, glassed in liquid nitrogen, and then introduced into the insert Dewar of the temperature controller in the EPR cavity. The *g* factors of the EPR spectra were determined by measuring the magnetic field displacement of the observed spectrum from the middle two lines of the six-line EPR spectrum of Mn^{2+} [16] in a solid SrO sample that was present in the EPR cavity at the same time as the measurements of the unknown spectrum.

Steady-state fluorescence and phosphorescence measurements were conducted with a cylindrical Pyrex tube (4-mm o.d.) inserted into a quartz Dewar filled with liquid nitrogen. The fluorescence and phosphorescence spectra were determined on a Perkin-Elmer Model MPF-4 spectrofluorometer.

Low-temperature fluorescence lifetime measurements were carried out with a cylindrical Pyrex tube (8-mm o.d.). For these measurements a Photochemical Research Associates Model 3000 nanosecond lifetime fluorometer[17] based on the technique of time-correlated single-photon counting[18] was used. A pulsed hydrogen arc lamp operated at ~30 kHz was used as the excitation source. The porphyrin concentrations were 10^{-6}–10^{-5} mol/L. In most experiments broad-band detection conditions[19] were employed by replacing the emission monochromator with either Corning CS 2-58 (640 nm) or CS 2-73 (580 nm) high-energy cutoff filters in the case of the experiments with a free base and metal–porphyrin samples, respectively. Fluorescence lifetimes and decay curves were obtained by computer deconvolution of each decay profile against the respective lamp profile obtained at the excitation wavelength. The χ^2 test and the appearance of random residues at the 95% confidence level were used as a criterion for goodness of fit.[17,18]

Results

When solutions of H_2TPP or H_2TTP in either the BuCl–CCl_4 or BuCl–TCE solvent mixtures were irradiated, the visible-region absorption bands located at about 650, 600, 550, and 525 nm in Figures 1a and 2a, respectively, decreased and new, more prominent absorption bands at about 675 and 445 nm appeared (Figures 1b and 2b). Identical absorption changes were obtained for irradiations with either near-UV (420 nm) or visible (515 nm) light, indicating that both the B-band and the Q-band regions were photoactive. The new visible-region spectra recorded near the end of the photolysis are shown as traces in Figures 1b and 2b for H_2TPP and H_2TTP, respectively, in a BuCl–TCE glass at 79 K. The complete photolytic conversion could not be easily obtained because of the very low quantum efficiency for these metal-free porphyrins.[1,2] Thus, complete-conversion spectra shown in Figures 1c and 2c were calculated by subtraction by computer of an estimated, residual amount of the spectrum of the parent porphyrin (Figures 1a and 2a) from the spectrum recorded following irradiation (Figures 1b and 2b). The calculations were based on an estimated photolytic conversion for each of the irradiated samples. The spectra of the products of the complete photolysis of both H_2TPP and H_2TTP in the alkyl chloride solutions (Figures 1c and 2c) share the same general features. These features include, in particular, the broad absorption bands that extend to 700 nm in the visible region and have been found to be common to the spectra of many metalloporphyrin π-cation-radical species (ref 14 and the ZnTPP π-cation-radical shown in Figure 3d).

Figure 3a shows the optical absorption spectra of ZnTPP in MTHF in the presence of 0.05 mol/L of DDQ at 79 K. The visible absorption spectra of ZnTPP in both neat MTHF and BuCl solvents are identical with the spectra of ZnTPP in the presence of the range of quinones used in this study. Specifically, there were no new absorption bands and no band broadening was detected; this indicates that this region of the ZnTPP spectrum is not influenced by the addition of the quinone acceptor. Figure 3b shows the optical absorption spectrum of the product of an exhaustive photolysis of ZnTPP in MTHF in the presence of 0.05 mol/L of DDQ at 79 K. The wavelength range selected for the irradiating light was limited by the cutoff at 410 nm in the blue and the attenuation of the infrared radiation obtained with the combination of the Corning CS 3-73 and a Corning CS 1-58 filters. Figure 3c shows the optical absorption spectrum of the product of an exhaustive photolysis of ZnTPP in a BuCl–CCl_4 glass at 79 K. These spectra of the low-temperature-photoxidized

(16) Bolton, J. R.; Borg, D. C.; Swartz, H. M. In "Biological Applications of Electron Spin Resonance"; Swartz, H. M., Bolton, J. R., Borg, D. C., Eds.; Wiley-Interscience: New York, 1972; p 100.
(17) Gudgin, E.; Lopez-Delgado, R.; Ware, W. R. *Can. J. Chem.* **1981**, *59*, 1037.
(18) Ware, W. R. In "Creation and Detection of the Excited State"; Ware, W. R., Ed.; Marcel Dekker: New York, 1971; Vol. 1, pp 213–301.
(19) Connolly, J. S.; Janzen, A. F.; Samuel, E. B., *Photochem. Photobiol.* **1982**, *36*, 559.

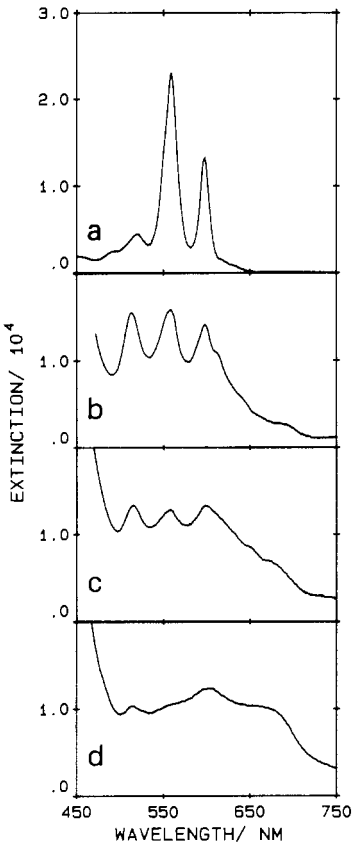

Figure 3. Visible region optical absorption spectra: (a) ZnTPP in MTHF containing 0.05 mol/L of DDQ at 79 K; (b) the product of an exhaustive photolysis of (a) at 79 K using light from a tungsten–halogen lamp filtered through Corning CS 3-73 and 1-58 filters; (c) $ZnTPP^{+\cdot}$ in a $BuCl–CCl_4$ (1:1 v/v) solution obtained by an exhaustive photolysis of the solution at 79 K; (d) $ZnTPP^+ClO_4^-$ formed chemically in CH_2Cl_2 at 298 K.[14]

ZnTPP (Figure 3b,c) differ from the room-temperature spectrum of the chemically oxidized ZnTPP (Figure 3d) in that there is an increase in the intensity of three bands between 500 and 600 nm and a decrease in intensity of the 680-nm band.

On the basis of these changes in the optical absorption spectrum, we can ascribe the product of ZnTPP photolysis in either the alkyl chloride solution or MTHF containing 0.05 mol/L of DDQ as a $ZnTPP^{+\cdot}$ π-cation-radical species. It is significant that even in the rigid matrix of the glass the photochemical oxidation of ZnTPP in MTHF in the presence of this quinone is reversible. Our experiments indicated that the neutral ZnTPP spectrum could be almost completely recovered following careful annealing of the irradiated MTHF solution between 95 and 100 K, i.e. about 30 K below the softening point of the solvent or following irradiation with broad-band infrared light in the spectral region where MTHF exhibits strong absorption (typically a Corning CS 2-58 (640 nm) high-energy cutoff filter can be used to perform such an experiment). If 0.05 mol/L of DDQ was replaced by 0.05 mol/L of p-Cl_4Q the yield of the $ZnTPP^{+\cdot}$ photochemical product was reduced substantially. There was no product yield if DDQ was replaced by up to even 0.5 mol/L of BQ.

Irradiated solutions of ZnTPP, H_2TTP, and MgTPP containing alkyl chlorides exhibit the EPR spectra presented in Figures 4a, 5a,c, and 6a, respectively. Each EPR spectrum shows a central, sharp singlet superimposed on a broader signal. When the irradiated solutions were warmed, the broad signal decayed, leaving only the sharp, symmetric signal, Figures 4b, 5b,d, and 6b, respectively. The thermal stability of the singlet spectrum depended on which porphyrin was being studied. Generally, the singlet spectrum of the free-base porphyrin, either H_2TTP or H_2TPP, was stable only in the rigid glass and decayed completely on warming above the liquid phase transition temperature, which was at about 180 K. The singlet EPR spectrum of ZnTPP (Figure 4b) was almost unchanged up to this temperature. With parameters of $g = 2.0024 \pm 0.0002$ and a peak-to-peak width of about 0.5 mT, this spectrum closely resembles that of $ZnTPP^{+\cdot}$ radicals obtained in liquid solution by both chemical and electrochemical oxidation.[20,21] The singlet EPR spectra of H_2TTP (Figure 5b,d) recorded between 140 and 150 K have similar characteristics, with a g factor of 2.0024 and a width of about 0.8 mT. These two species can then both be ascribed to the appropriate porphyrin π cation radicals.[20] In an attempt to obtain an increase resolution of the broad EPR signals observed in solutions containing CCl_4 (Figures 4a, 5c, and 6c), we used a crystalline matrix based on Me_4Si. Me_4Si solids are known to have a greater plasticity[22] relative to matrices based on BuCl and thus should allow greater movement within the lattice. However, there was no improvement in the resolution of the signal, and the EPR pattern remained the same in both the $BuCl–CCl_4$ and $Me_4Si–CCl_4$ solids. These results yield additional evidence that CCl_4 acts as the electron acceptor in low-temperature matrices. A computer plot of the broad signal that decays in a solution containing CCl_4 is presented in Figure 6e. This signal can be ascribed to the solvent radicals formed during the photochemical reaction.

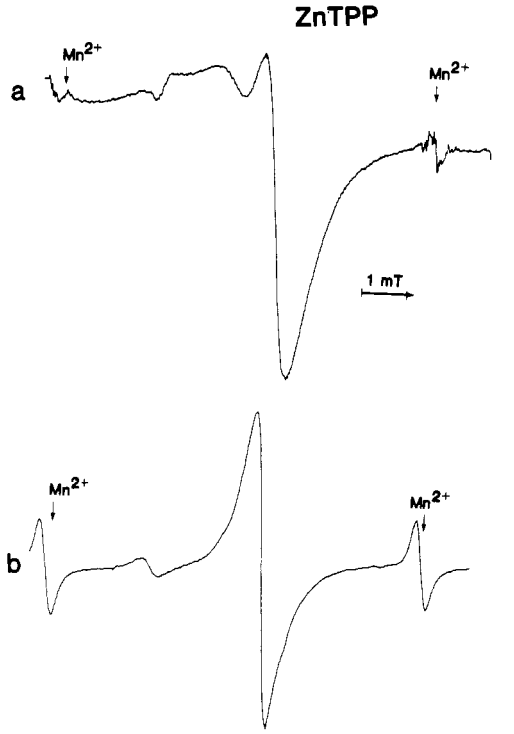

Figure 4. EPR spectra observed from the irradiation of ZnTPP in $BuCl–CCl_4$ (1:1 v/v): (a) at ~115 K; (b) after warming to ~150 K. The arrows mark the lines due to Mn^{2+}. EPR conditions: modulation amplitude 0.32 mT; microwave power 1 mW; at ~9.0 GHz.

Figure 7 shows fluorescence and phosphorescence spectra of ZnTPP in MTHF at 77 K, in the presence of various concentrations of added DDQ. It can be seen that the band positions of both fluorescence and phosphorescence spectra are unaffected by the presence of either DDQ, or any of the other quinones used in our studies. However, both fluorescence and phosphorescence intensities decrease exponentially with quinone concentration. This exponential dependence is illustrated in the semilog plots in Figure 8. These experimental results can be accounted for by assuming a critical quenching volume, V, such that luminescence intensity, I, is related to the critical quenching volume by a simple equation, which is described below as eq 10: $I/I_0 = e^{-VC}$, where I_0 is the

(20) Fajer, J.; Davies, H. S. In "The Porphyrins"; Dolphin, D., Ed.; Academic Press; New York, 1979; Vol. 4, pp 197–256.
(21) Fajer, J.; Borg, D. C.; Forman, A.; Felton, R. H.; Vegh, L.; Dolphin, D. *Ann. N.Y. Acad. Sci.* **1973**, *206*, 349.
(22) Westrum, E. F., Jr. *J. Chem. Educ.* **1962**, *39*, 443.

Table I. Energetics and Critical Quenching Radii, R_q, for the Reaction of ZnTPP* with Quinones in MTHF at 77 K

reaction	$E(*)^a$/eV	$\Delta G(P^+,Q^-)^b$/eV	$\Delta G(ET)^c$/eV	R_q/Å
ZnTPP (S) + BQ	2.05	1.23	−0.82	8.8
ZnTPP (T) + BQ	1.59	1.23	−0.36	8.9
ZnTPP (S) + p-Cl_4Q	2.05	0.63	−1.37	14.0
ZnTPP (T) + p-Cl_4Q	1.59	0.63	−0.91	14.5
ZnTPP (S) + o-Cl_4Q	2.05	0.54	−1.51	13.5
ZnTPP (T) + o-Cl_4Q	1.59	0.54	−1.05	13.0
ZnTPP (S) + DDQ	2.05	0.20	−1.85	20.0
ZnTPP (T) + DDQ	1.59	0.20	−1.39	24.5

[a] The first excited singlet (S) and triplet (T) state energy.[36] [b] $G(P^+,Q^-) = E(P^+/P) - E(Q/Q^-)$ in electronvolts, where $E(P^+/P)$ and $E(Q/Q^-)$ are the redox potentials measured in fluids. The ZnTPP redox potential, $E(P^+/P)$, is taken equal to 0.71 V (vs. SCE) in dichloromethane,[37] and the quinone redox potential, $E(Q/Q^-)$, has been assumed to have the value of −0.52, 0.03, 0.17, and 0.51 V (vs. SCE) for BQ, p-Cl_4Q, o-Cl_4Q, and DDQ in polar apriotic solvents,[38] respectively. The thermodynamic potential change for the back-electron-transfer reaction $P^{+}\cdot + Q^{-}\cdot \rightarrow P + Q$ can be approximated by $-\Delta G(P^+,Q^-)$. [c] Standard thermodynamic potential change for the ET reaction $P^* + Q \rightarrow P^{+}\cdot + Q^{-}\cdot$, approximated by $\Delta G(ET) = \Delta G(P^+,Q^-) - E(*)$. The actual values of $\Delta G(ET)$ in rigid MTHF may vary due to several factors.

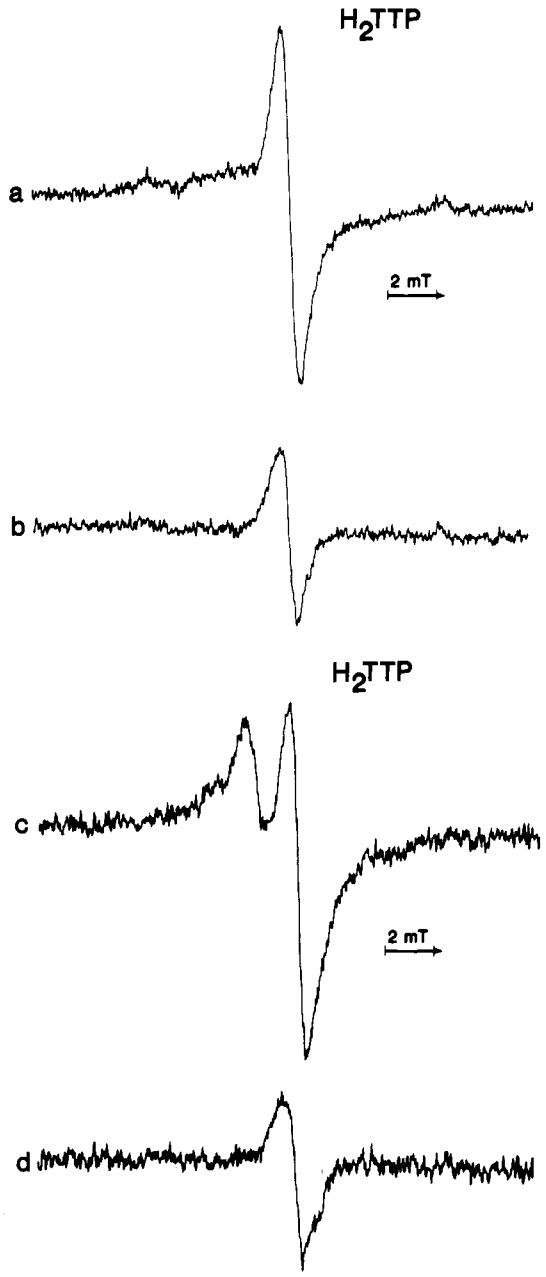

Figure 5. EPR spectra observed from irradiated solutions of H_2TTP: (a) TCE solution after irradiation at ~90 K; (b) the solution in (a) warmed to ~150 K; (c) BuCl–CCl_4 (1:1 v/v) solution irradiated at ~100 K; (d) the solution in (c) warmed to ~140 K. EPR conditions are as in Figure 4.

fluorescence intensity in the absence of the quencher and C is the quencher concentration. If the quenching volume is assumed to be spherical, then a critical quenching radius, R_q, can be calculated from the relationship $V = {}^4/_3\,\pi R_q^3$. Table I reports the observed quenching radii for the systems studied in this work.

Table II. Single-Exponential Analyses of the Fluorescence Decay Profiles for H_2TPP and ZnTPP in Alkyl Chloride Solutions at 77 K

porphyrin (soln)	λ_{exc}/nm	lifetime, t_0/ns	χ^2	time range[a]
TPP (BuCl)	420	14.51 ± 0.05	1.414	$0-\sim 2t_0$
	515	14.62 ± 0.05	1.635	
TPP (BuCl–CCl_4)	420	12.42 ± 0.05	1.405	$0-\sim 2t_0$
	515	12.29 ± 0.05	1.383	
ZnTPP (BuCl)	419	2.66 ± 0.01	0.906	$0-\sim 3.5t_0$
	555	2.76 ± 0.01	1.368	
ZnTPP (BuCl–CCl_4)	419	1.98 ± 0.01	1.683	$0-\sim 2t_0$
	555	2.10 ± 0.01	1.638	

[a] The largest initial time range where the single-exponential fits are satisfactory based on the χ^2 test and the appearance of random residuals at the 95% confidence level.

The fluorescence decay profiles for H_2TPP and ZnTPP in BuCl and BuCl–CCl_4 glasses at 77 K are shown in Figures 9 and 10, respectively. It is seen that fluorescence is quenched in glasses containing CCl_4. Excitation into either the B-band region or the Q-band region gives similar quenching results. However, the extent of quenching does differ for the two porphyrins analyzed. The results of the analysis of the fluorescence decay profiles are shown in Table II. A single-exponential fit was found to give a satisfactory deconvolution of the fluorescence decay for ZnTPP in the neat BuCl glasses at 77 K. A departure from the exponential decay has to be considered in the case of ZnTPP in a BuCl–CCl_4 (1:1 v/v) solution for the same time range. This departure is much less obvious in the case of H_2TPP in the same solvent mixtures due to the much reduced quenching effect.

Figure 11 shows fluorescence decay profiles for glassy samples at the liquid-nitrogen temperature of ZnTPP in MTHF and in MTHF containing various quinones. A single-exponential fit was found to give a satisfactory deconvolution of the fluorescence decay for ZnTPP in the absence of the quinones. The fluorescence profiles for ZnTPP in the presence of the quinones were found to deviate from the single-exponential decay curves. The character of this deviation depends on both the particular quinone and the specific concentration used. At minimum of two exponential components were needed to obtain satisfactory fits to these decay profiles, as shown in Table III. However, attempts to achieve consistent results by deconvolution of the decay profiles obtained using different concentrations of a given quinone were not successful. For example, the two-exponential function fits for solution containing different concentrations of BQ gave significant differences in the calculated lifetimes for the shorter and longer lived components (cf. Table III). One would expect that changes in the quencher concentration should only affect the contribution of each of the fluorescent components to the decay curves. Furthermore, deconvolution of the decay profiles over various time intervals for a given quencher concentration gave changes in both the lifetimes and contribution of the two fluorescent components. Thus, a two-exponential fit based on statistical criteria does not

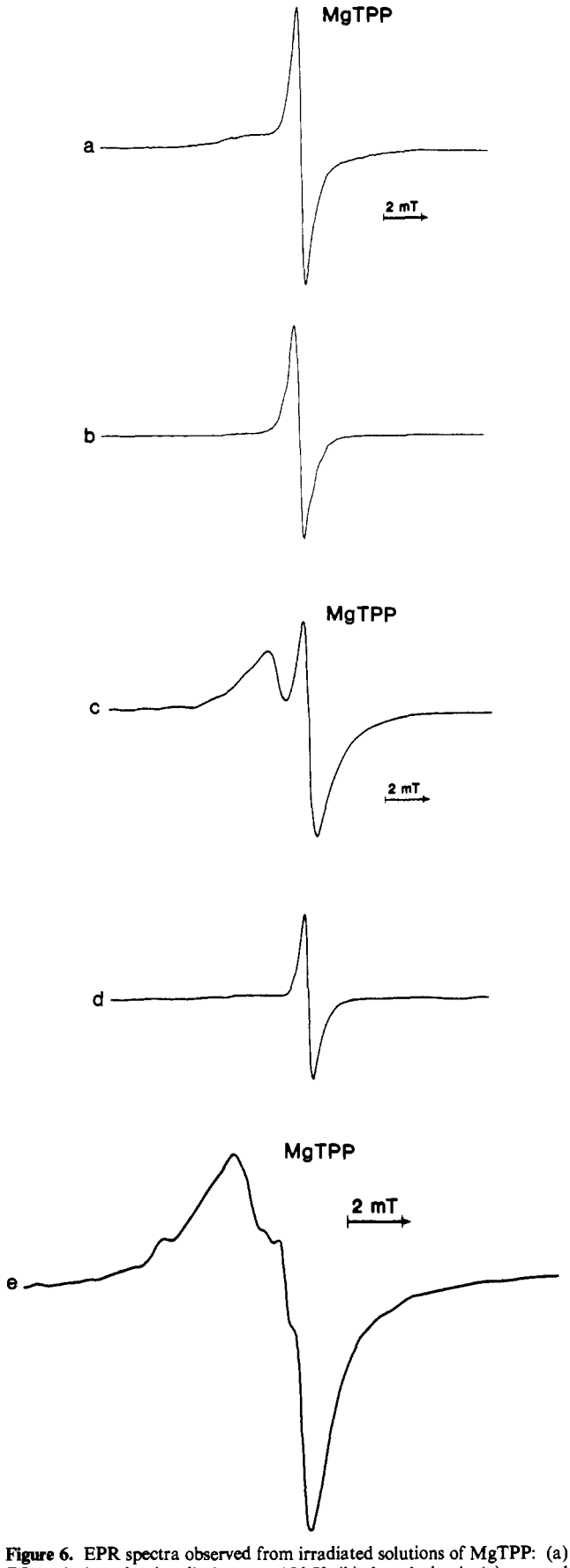

Figure 6. EPR spectra observed from irradiated solutions of MgTPP: (a) TCE solution after irradiation at ~100 K; (b) the solution in (a) warmed to ~180 K; (c) Me_4Si–CCl_4 (1:1 v/v) solution irradiated at 90 K; (d) the solution in (c) warmed to ~150 K; (e) digital subtraction of the spectrum recorded for MgTPP in BuCl–CCl_4 (1:1 v/v) at ~150 K from that obtained at ~90 K. The crossover point has g = 2.005. EPR conditions are as in Figure 4.

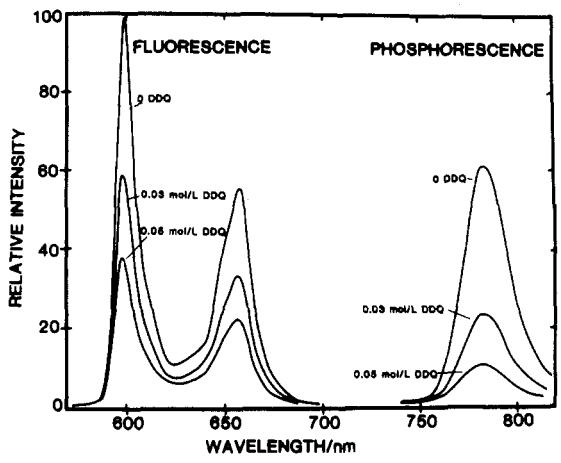

Figure 7. Fluorescence and phosphorescence spectra (uncorrected) of excited ZnTPP in MTHF at 77 K in the presence of various concentrations of DDQ. The excitation wavelength was 560 nm.

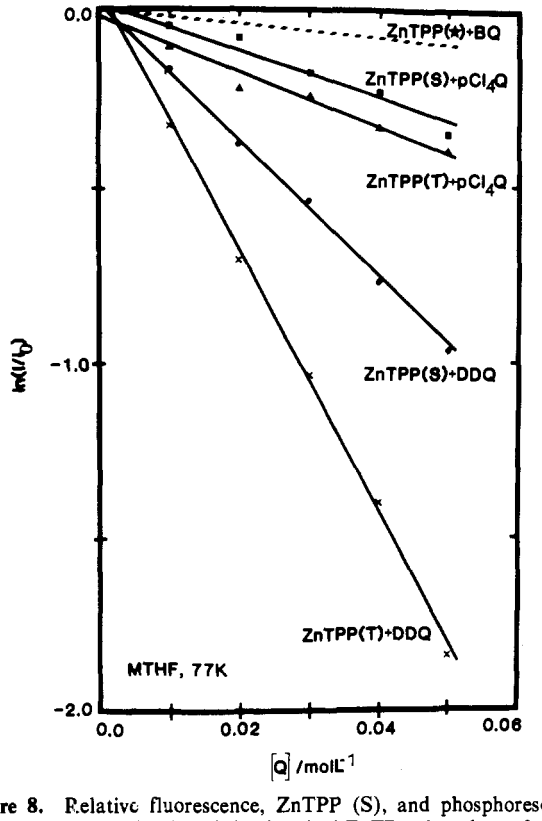

Figure 8. Relative fluorescence, ZnTPP (S), and phosphorescence, ZnTPP (T), intensities, ln (I/I_0), of excited ZnTPP plotted as a function of quinone concentration in MTHF at 77 K. The luminescence intensities for solutions containing BQ are approximately indicated by one broken line. The solid lines are least-squares fits to the experimental data.

Table III. Double-Exponential Analyses of the Fluorescence Decay Profiles for ZnTPP in Neat MTHF and in MTHF Containing Quinones at 77 K

quinone (concn/mol/L)	λ_{exc}/ nm	A_1/ %	t_1/ns	A_2/ %	t_2/ns	χ^2
	419			100	2.79 ± 0.01	1.25
	555			100	2.75 ± 0.02	1.11
BQ (0.2)	419			100	2.75 ± 0.01	1.47
BQ (0.2)	555	37	1.8 ± 0.5	63	3.0 ± 0.2	1.03
BQ (0.3)	419	35	0.83 ± 0.1	65	2.91 ± 0.02	1.46[a]
BQ (0.4)	419	47	0.63 ± 0.1	53	2.89 ± 0.02	1.25[a]
BQ (0.4)	555	56	0.9 ± 0.1	44	3.10 ± 0.05	1.20[a]
p-Cl_4Q (0.05)	555	46	1.4 ± 0.1	54	3.20 ± 0.06	1.18
o-Cl_4Q (0.1)	555	69	0.27 ± 0.13	31	2.69 ± 0.03	1.03
DDQ (0.05)	555	74	0.53 ± 0.04	26	2.90 ± 0.02	1.05

[a] The data do not fulfill the random residues criterion for goodness of fit.

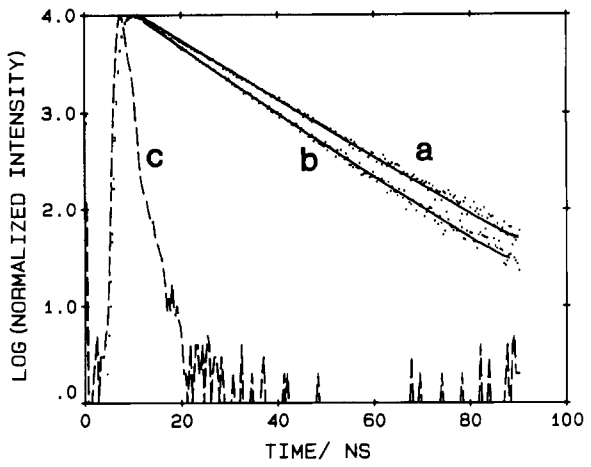

Figure 9. Fluorescence decay profiles obtained from $\sim 10^{-5}$ M solutions of H_2TPP excited at 420 nm in BuCl (a) and in BuCl–CCl_4 (1:1 v/v) (b) at 77 K together with a respective lamp profile (c). Solid lines represent fits to the fluorescence decay profiles or H_2TPP in BuCl (a) and in BuCl–CCl_4 (1:1 v/v) (b) by the general equation for the fluorescence decay: $J/J_0 = P(t)\ e^{-t/t_0}$. Parameters: $t_0 = 14.5$ ns, $P(t) = 1.0$ for H_2TPP (a); $t_0 = 14.5$ ns, $P(t) = e^{-(4/3)\pi C(L/2)^3[(\ln \nu t)^3+1.732(\ln \nu t)^2+5.934(\ln \nu t)+5.444]}$, with $L = 1.8$ Å and $\nu = 3 \times 10^8$ s^{-1} (b).

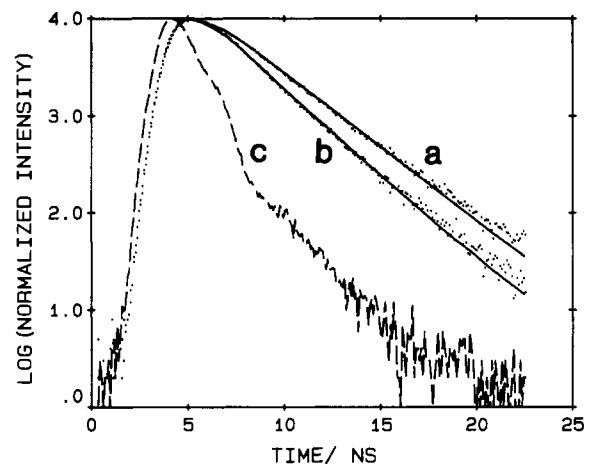

Figure 10. Fluorescence decay profiles obtained from $\sim 10^{-5}$ M solutions of ZnTPP excited at 419 nm in BuCl (a) and in BuCl–CCl_4 (1:1 v/v) (b) at 77 K together with a respective lamp profile (c). Solid lines represent fits to the fluorescence decay profiles for ZnTPP in BuCl and in BuCl–CCl_4 (1:1 v/v) by a general equation for the fluorescence decay: $J/J_0 = P(t)\ e^{-t/t_0}$. Parameters: $t_0 = 2.66$ ns, $P(t) = 1.0$ (a); $t_0 = 2.66$ ns, and $P(t)$ of the same general form as in Figure 9 with $L = 1.54$ Å and $\nu = 10^{10}$ s^{-1} (b).

necessarily seem to provide physically significant lifetime data. This means that a more general, nonexponential equation should be taken into account to explain the decay kinetics.

Discussion

The data presented above indicate that both free base and metalloporphyrins can be photooxidized in alkyl chloride solutions containing TCE or CCl_4 to form porphyrin π-cation-radical species. It is suggested that the lowest singlet excited state is likely to be directly involved in the electron transfer from the photoexcited porphyrin to the polychloride alkane acceptors. The experimental results can be explained by the simple reaction scheme (1)–(3), where P, P* and $P^{+}\cdot$ are the ground-state,

$$P^* \rightarrow P \quad (1)$$

$$P^* + RCl \rightarrow P^{+}\cdot + (RCl)^{-}\cdot \quad (2)$$

$$(RCl)^{-}\cdot \rightarrow R\cdot + Cl^- \quad (3)$$

electronically excited-state, and π-cation-radical porphyrins, respectively, and RCl is the alkyl chloride acceptor (CCl_4 or TCE).

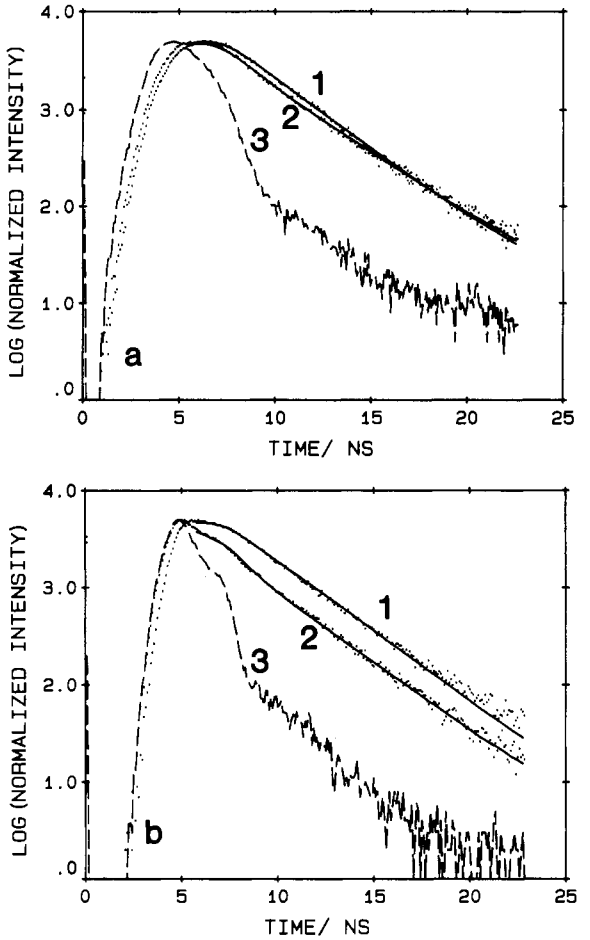

Figure 11. Fluorescence decay profiles obtained at 77 K from $\sim 10^{-5}$ mol/L solutions of ZnTPP excited at 555 nm in MTHF (1) and in the presence of quinones (2), together with respective lamp profiles (3): (a) 0.4 mol/L of BQ; (b) 0.05 mol/L of DDQ. Analyses of these profiles by computer deconvolution are presented in Table III.

The absorption and EPR spectra of the π cation radicals $P^{+}\cdot$ of the free base, zinc, and magnesium porphyrins appear to reflect the $^2A_{2u}$ character of their electronic ground state.[14,20,21] The observed spectral differences in Figure 3b–d for the oxidized ZnTPP species may reflect more than differences in the type of ligand complexed to the porphyrin, for the room-temperature spectrum of the photooxidized ZnTPP complex is similar to the spectrum of the chemically oxidized porphyrin (Figure 3d) except for a reduction of intensity in the 680-nm band. In contrast, there are three well-resolved bands in the 500–600-nm region of the spectra in Figure 3b,c of $ZnTPP^{+}\cdot$ in a rigid solution when compared to the room-temperature spectrum of $ZnTPP^{+}\cdot$ (Figure 3d). These differences may be due to a "cage" interaction between the spins located on the porphyrin radicals and the nearby acceptor radical or to a strained conformation of the oxidized porphyrin in the rigid matrix.

The EPR signal of solvent radicals in irradiated glasses containing CCl_4 shows striking similarity to the EPR spectrum of $CCl_3\cdot$ radicals obtained by different means (cf. ref 23). The broad EPR signal obtained for glasses containing TCE (Figures 5a and 6a) may be tentatively assigned to $CHCl_2CHCl\cdot$ radicals. The broad EPR spectrum does not represent $Cl_2^{-}\cdot$ radicals, as might be predicted from the one-electron-extrusion reaction $CHCl_2CHCl_2 + e^- \rightarrow CHCl{=}CHCl + Cl_2^{-}\cdot$[23] nor can it represent the $CHCl_2CHCl_2^{-}\cdot$ anion radical, since such a radical is known to be photolabile.[24] The poor resolution observed in the EPR spectra of the alkyl chloride radical is consistent with data obtained for

(23) Mishra, S. P.; Symons, M. C. R. *Faraday Soc. Discuss.* **1977**, *63*, 175.
(24) Hesagawa, A.; Shiotani, M.; Williams, F. *Faraday Soc. Discuss.* **1977**, *63*, 157.

other polyhalogenated alkane radicals.[24]

The shortened fluorescence lifetimes for both H_2TPP and ZnTPP in glasses containing CCl_4 (Table II) implies quenching, which arises from electron transfer from the lowest singlet excited state of the porphyrin to the alkyl chloride acceptor. For the MTHF solutions containing quinones the experimental results can be interpreted in terms of the electron-transfer reactions (4) and (5). The experimental data of the observed emission quenching can only be explained in terms of the electron-transfer mechanism for this type of reaction scheme.

$$P^* + Q \rightarrow P^{+\cdot} + Q^{-\cdot} \quad (4)$$

$$P^{+\cdot} + Q^{-\cdot} \rightarrow P + Q \quad (5)$$

In addition, the product of the photochemical reaction (4) of ZnTPP has been stabilized for the first time at high yield under appropriate thermodynamic conditions that allow for both reactions 4 and 5 to occur. It should be noted that both the forward ET reaction, involving the first singlet and triplet excited states of ZnTPP, and the back ET reaction between the ground-state $ZnTPP^{+\cdot}$ cation radical and a number of quinone anion radicals $Q^{-\cdot}$ are accessible on thermodynamic grounds (cf. Table I). The ET theories[25,26] and reported experimental data[27-29] indicate that the rate of ET reactions decreases rapidly when thermodynamic potential, $\Delta G(ET)$, approaches zero, especially at low temperatures. An experimentally observed threshhold of the $\Delta G(ET)$ at low temperatures for the ET reactions was reported to be of about -0.5 eV.[27] Thus, favorable conditions for stabilization of the radical ions should occur for the donor–acceptor pair with a relatively low negative $\Delta G(ET)$ for the back-reaction (5). In agreement with this prediction the charge-separated product is stabilized following photolysis in MTHF at liquid-nitrogen temperatures at a high yield in the ZnTPP–DDQ mixture, and no accumulation of a photochemical product is observed in the case of ZnTPP–BQ. On the other hand, there should be no back-reaction in the photolyzed solutions containing the alkyl chloride acceptor, as there is now a nonreversible, dissociative decay of the primary anion radical of the acceptor (reactions 2 and 3). This process will allow for the accumulation of the oxidized porphyrin species if the thermodynamic requirements of the forward reaction involving the excited porphyrin molecules are favorably fulfilled.

If the luminescence is assumed to be quenched by electron transfer from the P* to RCl (reaction 2) or Q (reaction 4), which competes with the radiative decay (reaction 1), an exact mathematical expression for the decay function of the donor luminescence for the volumeless, randomly distributed donor and acceptor molecules can be obtained. The function has the simplified general form in (6), where $P(t)$ is the time-dependent

$$I(t)/I_0 = P(t)\, e^{-t/t_0} \quad (6)$$

component of the decay function due to the competitive electron-transfer reaction and t_0 is the luminescence lifetime. $P(t)$ for the electron-transfer quenching can be obtained in a mathematical analogy to the treatment of Inokuti and Hirayama[30] of the triplet–triplet excitation transfer, which is based on the electron-exchange mechanism[31] in (7), where $f(vt)$ can be

$$P(t) = e^{-(4/3)\pi C(L/2)^3 f(vt)} \quad (7)$$

approximated for $vt > 10$ by the function in (8). Alternatively,

$$f(vt) = (\ln vt)^3 + 1.732(\ln vt)^2 + 5.934(\ln vt) + 5.444 \quad (8)$$

the luminescence decay function, which also takes into account the finite size of the reactants, can be derived in a mathematical form as proposed by Miller[27,32] for electron-transfer reactions in rigid, homogeneous solutions (eq 9). In both expressions, C is

$$P(t) = e^{-(4/3)\pi C\{[R_0+(L/2)(\ln vt)]^3-R_0^3\}} \quad (9)$$

the acceptor concentration, L is a range parameter, and v is a frequency factor defined by a general expression for the distance dependence of the rate constant of the electron-transfer reaction: $k(R) = ve^{-2R/L}$.[25,26] R_0 is the center-to-center distance when the electron donor and acceptor are in contact.

Both models predict that the results of the steady-state emission quenching can be interpreted by a simple capture–volume model first proposed by Perrin[33] that describes the exponential dependence of the donor luminescence intensity on the acceptor concentration:

$$I/I_0 = e^{-VC} \quad (10)$$

As a result R_q (Table I) is interpreted as the critical electron-transfer distance at which the electron transfer occurs with the same rate as the radiative decay such that at $R < R_q$ the emission is totally quenched, while for $R > R_q$ the excited-state emission is unperturbed, with R_q recognized here as an average quantity. Thus, the exponential decrease in intensity of both the fluorescence and phosphorescence of ZnTPP with the concentration of quinone (cf. Figure 8) is in agreement with the electron-transfer mechanism. Moreover, the efficiency of quenching correlates well with calcualted energetics for electron transfer from the excited donor to the added acceptor. This model predicts that there will be larger R_q values for quenching excited states that have longer lifetimes (cf. millisecond phosphorescence lifetimes and nanosecond fluorescence lifetimes). The alternative quenching mechanism by the intersystem crossing (ISC) enhancement can be rejected on the grounds that the phosphorescence quenching is more efficient than fluorescence, especially in the case of chlorinated *p*-quinones, where the ISC mechanism could play a role by the external, heavy-atom effects of the chlorine groups. The electronic energy-transfer mechanisms can be neglected since the overlap between the ZnTPP emission spectrum and the absorption spectrum of the quinones is extremely small. The observed emission quenching is also less likely due to the donor–acceptor complexation. No new absorption or emission bands were observed in any of the ZnTPP–Q systems when compared to the ZnTPP solution, within the concentration range employed. Formation of nonemissive charge-transfer complexes should result in a Stern–Volmer type dependence of the emission intensity on the quencher concentration. We do not observe such a dependence in the experimental data. Furthermore, the quenching efficiency should not depend on the excitation energy $E(^*)$ or the excited-state lifetime in a complexation mechanism; such a mechanism would fail to explain the uneven quenching effects observed for phosphorescence and fluorescence intensities. In addition, a complexation mechanism resulting in static fluorescence quenching should not give changes in the fluorescence decay rate.

The electron-transfer mechanism predicts a nonexponential, faster decay of donor luminescence in a homogeneous, diffusionless system. The fluorescence decay curves for both the H_2TPP and ZnTPP in BuCl containing 50% (v/v) of CCl_4 can be fitted to a nonexponential decay function (eq 6) by eq 7 and 8 (cf. Figures 9 and 10). The existence of the nonexponential kinetics for the fluorescence decay of indole in rigid solution containing alkyl chlorides has been shown[34] to indicate the direct involvment of the electron transfer from the singlet excited state, while an alternative quenching mechanism involving the enhancement of intersystem crossing by the external heavy-atom effect of chlorine was excluded.

The statistically significant departure from single-exponential kinetics for the fluorescence decay has been found for all ZnTPP–quinone systems studied in this work. The nonexponential

(25) Jortner, J. A. *J. Am. Chem. Soc.* **1980**, *102*, 6676.
(26) Markus, R. A.; Siders, P. *J. Phys. Chem.* **1982**, *86*, 622.
(27) Miller, J. R.; Peeples, J. A.; Schmitt, M. J.; Closs, G. L. *J. Am. Chem. Soc.* **1982**, *104*, 6488.
(28) Guarr, T.; McGuire, M.; Strauch, S.; McLendon, G. *J. Am. Chem. Soc.* **1983**, *105*, 615.
(29) Beitz, J. V.; Miller, J. R. *J. Chem. Phys.* **1979**, *71*, 4579.
(30) Inokuti, M.; Hirayama, F. *J. Chem. Phys.* **1965**, *43*, 1978.
(31) Dexter, D. L. *J. Chem. Phys.* **1953**, 21, 836.
(32) Miller, J. R.; Hartman, K. W.; Abrash, S. *J. Am. Chem. Soc.* **1982**, *104*, 4298.
(33) Perrin, F. *C. R. Hebd. Seances Acad. Sci.* **1924**, *178*, 1978.
(34) Namiki, A.; Nakashima, N.; Yoshihara, K. *J. Chem. Phys.* **1979**, *71*, 925.

fluorescence decay for certain ruthenium complexes in the presence of an electron acceptor in a rigid solution has been recently interpreted[28,35] in terms of an electron-transfer mechanism. We have attempted to fit our experimental decay data for the quinone acceptors to the decay function (6), using $P(t)$ derived from both models, although, unlike fluorescence decay with the CCl_4 acceptor no reasonable values for the parameters v and L were obtained from the analyses for the range of quinones used. The failure to find satisfactory fits of these data to function 6 is likely due to neglecting to include in the calculation the effect of molecular orientation on the electron transfer. Likewise, in the reported analyses[29,34,35] of the electron-transfer reactions in rigid solutions, the effects of molecular orientation on ET rates were also neglected, and the measured rate constants were orientation-averaged quantities. The orientation-dependent ET rate constants, which differ by more than 1 order of magnitude, are suggested in studies of linked PQ molecules;[12] it seems likely that the ET rate will decrease 1 order of magnitude or more for the most unfavorable orientation. Also, if ET is fast enough on a fluorescence time scale, a departure from the random P–Q distribution kinetics is likely to be observed. Therefore, we conclude that the failure to find a suitable kinetic equation for the fluorescence decay for ZnTPP in glassy MTHF solutions containing quinones can be attributed to the orientation effect in this electron-transfer reaction in the diffusionless system. This effect should be more pronounced in the case of the quinone acceptor than in the case of the alkyl chloride acceptor due to the more rigorous structural requirements for electron transfer in the former case.

Acknowledgment. The authors gratefully acknowledge the financial support of this work by the NSERC of Canada through grants under the Operating Equipment and Strategic (Energy) programs (to M.J.S.) and by the Centre for Interdisciplinary Studies in Chemical Physics for a Visiting Fellowship (to Z.G.). We also thank Dr. Alan R. McIntosh for the assistance with the EPR experiments. The authors are associated with the Centre for Chemical Physics at the UWO.

(35) Strauch, S.; McLendon, G.; McGuire, M.; Guarr, T. *J. Phys. Chem.* **1983**, *87*, 3579.
(36) Darvent, J. R.; Douglas, P.; Harriman, A.; Porter, A.; Richoux, M.-C. *Coord. Chem. Rev.* **1982**, *44*, 83.
(37) Felton, R. H. In "The Porphyrins"; Dolphin, D., Ed.; Academic Press: New York, 1978; Vol. 5, pp 53–115.
(38) Mann, C. L.; Barnes, K. K. In "Electrochemical Reactions in Nonaqueous Systems"; Marcel Dekker: New York, 1970.

Contribution from the Department of Chemistry, University of California, Berkeley, California 94720

Lipophilic Enterobactin Analogues.[1] Stabilities of the Gallium and Ferric Ion Complexes of Terminally N-Substituted Catechoylamides

MARY J. KAPPEL, VINCENT L. PECORARO, and KENNETH N. RAYMOND*

Received September 7, 1984

The formation constants and metal complex protonation behavior of four lipophilic N-substituted tricatechoylamide analogues of enterobactin with Fe^{3+} and Ga^{3+} have been evaluated. The ligands *N,N''*-diisopropyl-*N,N',N''*-tris(5-sulfonato-2,3-dihydroxybenzoyl)-1,5,10-triazadecane (DiP-3,4-LICAMS), *N,N''*-dibenzyl-*N,N',N''*-tris(5-sulfonato-2,3-dihydroxybenzoyl)-1,5,10-triazadecane (DB-3,4-LICAMS), *N,N''*-dicyclohexyl-*N,N',N''*-tris(5-sulfonato-2,3-dihydroxybenzoyl)-1,5,10-triazadecane (DC-3,4-LICAMS), *N,N',N''*-triisopropyl-*N,N',N''*-tris(5-sulfonato-2,3-dihydroxybenzoyl)-1,3,5-tris(aminomethyl)benzene (TiP-MECAMS) all form tris(catecholato) Fe^{3+} and Ga^{3+} complexes. Comparison of the metal complex stabilities of the N-substituted ligands to those of the nonlipophilic 3,4-LICAMS and MECAMS indicates that the ferric complexes are of similar stability; the gallium complexes are significantly less stable.

Introduction

Interest in the development of new iron chelating agents for their potential medical application in ferric ion decorporation therapy for persons with β-thalassemia[2,3] has spurred a program of ligand design and synthesis.[4,5] These synthetic ligands have also been used as chelating agents for Ga(III) and In(III),[6] since Ga(III) in particular is almost identical with Fe(III) in size.[7] Radiopharmaceuticals incorporating ^{67}Ga and ^{111}In are used for imaging abscesses and tumors.[8] Hexadentate ligands are designed to chelate excess ^{67}Ga(III) or ^{111}In(III) in the bloodstream, thus improving the tumor or abscess image and decreasing exposure of the patient to unnecessary radiation.[6,9]

Recognizing that microbes produce a hexadentate ligand, enterochelin[10] (enterobactin[11]), capable of effectively sequestering ferric ion,[12] a design concept was conceived to modify the hydrolytically unstable ester-linked backbone of enterobactin while preserving the ligand's inherent specificity for ferric ion as well as its stability.[13,14] Subsequent modifications have been to sulfonate[15] or carboxylate[16] the catechol rings to increase water solubility and decrease oxidation of the ligand by oxygen. Another modification seeks to increase the lipophilicity of the ligand by attaching organic moieities to the amide nitrogen.[17] This should change the tissue distribution of the metal complex in vivo. Indeed, the derivative having an *n*-octyl chain attached to the amide nitrogen crosses the blood/brain barrier,[18] which is seldom pen-

(1) This is paper No. 12 in the series "Ferric Ion Sequestering Agents" and No. 4 in the series "Gallium and Indium Imaging Agents". For the previous papers in these series see respectively: Rodgers, S. J.; Raymond, K. N. *J. Med. Chem.* **1983**, *26*, 439; ref 9 of this paper.
(2) Andersen, W. F., Hiller, M. C., Eds. *DHEW Publ. (NIH) (U.S.)* **1975**, *NIH-77-994*.
(3) Jacobs, A. *Br. J. Haematol.* **1979**, *43*, 1.
(4) Martell, A. E.; Andersen, W. F.; Badman, D. G. "Proceedings from a Symposium on the Development of Iron Chelators for Clinical Use"; Elsevier North-Holland: New York, 1981; pp 165–187.
(5) Raymond, K. N.; Harris, W. R.; Carrano, C. J.; Weitl, F. L. *ACS Symp. Ser.* **1980**, *No. 140*, 313.
(6) Moerlein, S. M.; Welch, M. J.; Raymond, K. N.; Weitl, F. L. *J. Nucl. Med.* **1981**, *22*, 710.
(7) Shannon, R. D. *Acta Crystallogr., Sect. A: Cryst. Phys., Diffr., Theor. Gen. Crystallogr.* **1976**, *A32*, 751.
(8) Welch, M. J.; Moerlein, S. M. *ACS Symp. Ser* **1980**, *No. 140*, 121.
(9) Moerlein, S. M.; Welch, M. J.; Raymond, K. N. *J. Nucl. Med.* **1982**, *23*, 501.
(10) O'Brien, I. G.; Gibson, F. *Biochim. Biophys. Acta* **1970**, *215*, 393.
(11) Pollack, J. R.; Neilands, J. B. *Biochim. Biophys. Res. Commun.* **1970**, *38*, 989.
(12) Harris, W. R.; Carrano, C. J.; Raymond, K. N. *J. Am. Chem. Soc.* **1979**, *101*, 2213.
(13) Weitl, F. L.; Raymond, K. N. *J. Am. Chem. Soc.* **1979**, *101*, 2728.
(14) Harris, W. R.; Raymond, K. N. *J. Am. Chem. Soc.* **1979**, *101*, 6534.
(15) Weitl, F. L.; Harris, W. R.; Raymond, K. N. *J. Med. Chem.* **1979**, *22*, 1281.
(16) Weitl, F. L.; Raymond, K. N.; Durbin, P. W. *J. Med. Chem.* **1981**, *24*, 203.
(17) Weitl, F. L.; Raymond, K. N. *J. Org. Chem.* **1981**, *46*, 5234.

0020-1669/85/1324-2447$01.50/0